JOURNAL OF SOLID STATE CHEMISTRY 111, 111–117 (1994)

Ordered and Disordered Homologues of Orthorhombic Mo_4O_{11} in the Mo–W–O System

L. Kihlborg, B.-O. Marinder, M. Sundberg, F. Portemer,[1] and O. Ringaby

Department of Inorganic Chemistry, Arrhenius Laboratory, Stockholm University, S-106 91 Stockholm, Sweden

Received November 8, 1993; accepted February 18, 1994

IN HONOR OF C. N. R. RAO ON HIS 60TH BIRTHDAY

Homologues of the orthorhombic form of Mo_4O_{11}, belonging to the series $M_{m+2}O_{3m+4}$, have been prepared in the Mo–W–O system and structurally characterized by X-ray powder diffraction and electron microscopy. The structures are built up of corner-sharing MO_6 octahedra in ReO_3-type slabs of characteristic width m and alternatingly mirrored orientation, connected by MO_4 tetrahedra along planes where pentagonal tunnels are formed. The structures can be designated by $[m,\bar{m}]$. The phases $(Mo,W)_4O_{11}$, $(=[6,\bar{6}])$, and $(Mo,W)_9O_{25}$ $(=[7,\bar{7}])$ were obtained almost pure and slabs of other widths, intergrown in more or less disordered fashion, were frequently observed by HREM. Slabs in parallel orientation, as in Mo_4O_{11}(mon), have also been seen, as well as a coherent boundary across which the structure $[6,\bar{6}]$ changes into $\sim[5,\bar{7}]$.

INTRODUCTION

The reduced oxide Mo_4O_{11} occurs in two modifications; one with a monoclinic structure that forms below ~600°C and the other with an orthorhombic lattice obtained above that temperature (1). The structures of these are similar; both consist of slabs of the ReO_3 type cut parallel to {211}, six octahedra wide along two subcell axes and mutually connected by MoO_4 tetrahedra across the slab boundaries, as shown in Fig. 1. They differ in the relative orientation of the slabs; in the monoclinic form (2) all the slabs are in the same orientation, while in the orthorhombic modification (2–4) every second slab is mirrored. Both modifications can be considered as members of homologous series (2), with the general formula $M_{m+2}O_{3m+4}$, where the members differ in the width of the slabs, expressed in terms of the number of octahedra, m (Fig. 1). The ordered stacking sequence can conveniently be expressed by $[m]$ for the monoclinic series and $[m,\bar{m}]$ for the orthorhombic one. This also allows more complex stackings to be described. The two Mo_4O_{11} $(=Mo_8O_{22})$ phases both have $m = 6$ and should thus be designed [6] and $[6,\bar{6}]$.

No other members of these series have been prepared in the binary Mo–O system. It was recently found, however, that if some molybdenum is replaced by tungsten, homologues of the monoclinic form can be synthesised (5). By gentle reduction at 350°C of the mixed ReO_3-type oxide $Mo_{0.72}W_{0.28}O_3$, the ordered members [7] and [8] were thus obtained and disordered fragments with m values ranging from 2 to 9 were observed by high-resolution electron microscopy (HREM).

Among the *monophosphate tungsten bronzes*, extensively investigated by the Caen group, the members of the "$MPTB_P$" family are isostructural with the orthorhombic $[m,\bar{m}]$ phases (6–11). The general formula of these is $(PO_2)_2(WO_3)_m$ and PO_4 tetrahedra replace the MoO_4 tetrahedra in Mo_4O_{11}(o-rh). Phases with m values ranging from 2 to 11 have been prepared, while crystallites or microphases representing even higher members have been observed by HREM (7, 9). The member $m = 5$ forms a notable exception as its structure turned out to be $[4,\bar{6}]$ rather than $[5,\bar{5}]$ (7). Phosphate niobium bronzes, $A_x(PO_2)_2(NbO_3)_m$, of the same structure type but with alkali in the pentagonal tunnels, have also been prepared recently (12–14). Monophosphate tungsten bronzes of the monoclinic series, represented by $[m]$, are also known, but only with alkali in the hexagonal tunnels (see Ref. (15) for a review).

The two Mo_4O_{11} modifications, as well as the purple molybdenum bronzes, $A_{0.9}Mo_6O_{17}$, with a related structure, have attracted considerable interest in the last years because of their quasi-two-dimensional electrical transport properties and charge density wave instabilities (16).

We have made preparations of samples in the Mo–W–O system by conventional high-temperature synthesis and found ordered and disordered homologues of the orthorhombic series, which are reported below. Some preliminary results were presented at SCANDEM 93 (17).

[1] On leave from Laboratoire de Réactivité et de Chimie des Solides, URA CNRS 1211, Université de Picardie, Amiens, France.

0022-4596/94 $6.00

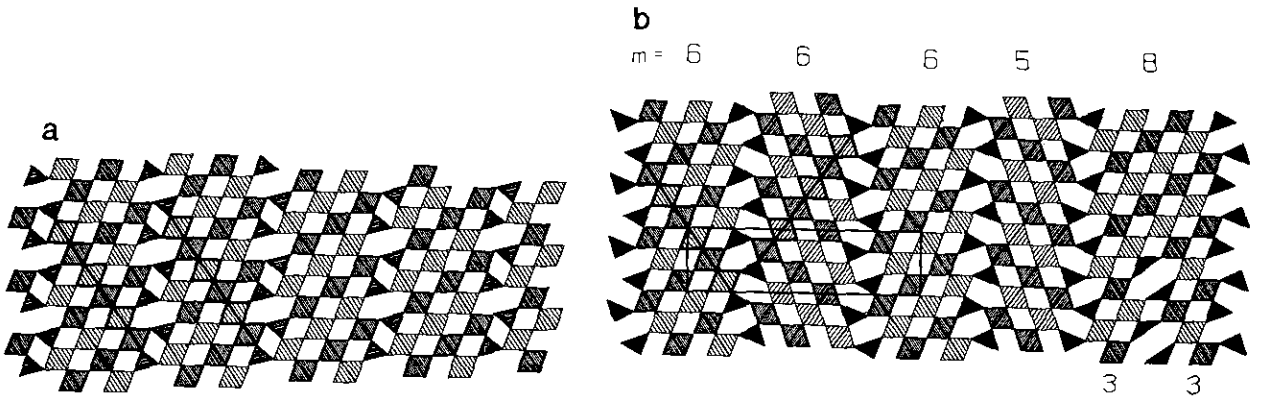

FIG. 1. Idealized structure models of monoclinic (a) and orthorhombic (b, left part) Mo_4O_{11} seen along [010] with a ~5.4-Å repeat. Octahedra at two levels, differently shaded, are connected by corners to form ReO_3-type slabs, infinite in two dimensions. The slabs are connected by tetrahedra at two levels (shown as triangles) along vertical planes, giving rise to "hexagonal" tunnels in the monoclinic form and "pentagonal" ones in the orthorhombic. In (b) the orthorhombic unit cell is outlined (*a*, horizontal; *c*, vertical). The width of the slabs can be expressed by the number of octahedra, *m*, along strings, two of which are heavily outlined in each model. In both these structures $m = 6$. In the right part of (b) slabs of different widths are shown. The rightmost slab, with $m = 8$, is moreover split in its lower part into two slabs with $m = 3$, resulting in a local intergrowth of the monoclinic structure. To correspond to the HREM observations it must be assumed that the real structure relaxes around this defect.

EXPERIMENTAL

One sample (*A*) of composition $Mo_{7.3}W_{1.7}O_{25}$ was prepared from a mixture of appropriate amounts of MoO_2, MoO_3 and WO_3. Two other samples (*B* and *C*) were made with the composition Mo_3WO_{11}. *B* was prepared from MoO_3, WO_3, and W metal powder, while Mo metal was used instead of W for sample *C*. The finely ground mixtures were enclosed in silica tubes that were evacuated and heated in a programmable furnace at 600°C (*A* and *B*) or 400°C (*C*) for 1 day and at 800°C for 3 days and then cooled at a rate of 300°C/hr. It was noted that a slight escape of MoO_3 from the reaction mixtures had taken place as a crystalline deposit was observed at the top of the silica tubes.

The samples were investigated by recording their X-ray powder diffraction patterns at room temperature in a Guinier–Hägg focusing camera using $CuK\alpha_1$ radiation and Si as an internal standard ($a = 5.4301$ Å). The films were evaluated in an automatic film scanner system (18).

HREM studies were made at 200 kV accelerating voltage in a JEOL JEM-200CX transmission electron microscope equipped with a double-tilt, top-entry specimen stage. The specimens were crushed in a mortar, dispersed in *n*-butanol, and collected on holey carbon films supported by copper grids. Images were simulated using a local version of the multislice program suite SHRLI (19).

RESULTS

It was clear from the appearance of electron diffraction (ED) patterns and HREM images of the samples that they contained ordered crystals of the $[6,\bar{6}]$ and $[7,\bar{7}]$ homologues. In addition, other sequences as well as defects and disordered crystallites were occasionally found, as will be described in a subsequent section. Given this evidence, the X-ray diffraction patterns could be evaluated and the main constituents identified.

Sample *A* showed an almost single-phased pattern very similar to that of orthorhombic Mo_4O_{11} with the unit-cell dimensions $a = 24.505(3)$ Å, $b = 5.4608(6)$ Å, $c = 6.7589(6)$ Å, $V = 904.5$ Å^3. These values can be compared with the cell dimensions of the pure molybdenum oxide, $a = 24.4726(15)$ Å, $b = 5.4567(3)$ Å, $c = 6.7510(6)$ Å, $V = 901.51$ Å^3. The substitution of tungsten for ~20% of the molybdenum in Mo_4O_{11}(o-rh) thus causes a ~0.3% increase of the unit cell.

Sample *B* was found to be a mixture of phases. One of these was $(Mo,W)_4O_{11}$(o-rh), identical with the one found in sample *A*. A second phase was the $[7,\bar{7}]$ homologue, i.e., $(Mo,W)_9O_{25}$(o-rh), with the unit-cell dimensions $a = 27.641(4)$ Å, $b = 5.4474(5)$ Å, $c = 6.7369(7)$ Å, $\alpha = 90.20(1)°$, $V = 1014.4$ Å^3. Traces of MoO_2 were also found. The unit-cell dimensions of the Mo_4O_{11}-type, $[6,\bar{6}]$-phase were practically the same as those in *A*.

Sample *C* of the same overall composition contained mainly $(Mo,W)_9O_{25}$(o-rh) in addition to traces of MoO_2. The $[7,\bar{7}]$-phase had the unit-cell dimensions $a = 27.632(5)$ Å, $b = 5.4453(6)$ Å, $c = 6.73767(7)$ Å, $\alpha = 90.17(2)°$, $V = 1013.8$ Å^3. The small monoclinic distortion of the lattice of this phase, in contrast to that of $[6,\bar{6}]$, was clearly evidenced in the powder patterns and has also been found in a single-crystal investigation (20). This deviation from orthorhombic symmetry was too small to be obvious in the ED patterns. (It has not yet been possible

to record convergent beam patterns of these crystallites.) The unconventional setting of the cell is chosen to keep the axes orientation the same for all these phases.

Our ED studies revealed that all samples also contained minor fractions of crystallites with a crystallographic shear (*CS*) structure, $(Mo,W)_nO_{3n-1}$, with n = 10–12 (21).

Typical ED patterns of the [7,$\bar{7}$] phase in three projections and, for comparison, also one of the [6,$\bar{6}$] phase in [001] orientation, are shown in Fig. 2. There are distinct features in all these projections to make identification easy. The difference is particularly marked in the [001] projection (with a pseudo-hexagonal subcell), where the a axis due to the symmetry appears halved in the even-m members but not in those with odd m. In this projection the number of (possible) spots along a^* between the strong sublattice reflections is $(m + 1)$ for the even-m members and $(2m + 3)$ for the odd members.

An HREM image of an ordered crystal of the [7,$\bar{7}$] phase in [010] projection is shown in Fig. 3 with a simulated image inserted. The straight strings of seven octahedra connected by tetrahedra form a typical zigzag pattern of dots, which are just at the limit of resolution in this projection. The pentagonal tunnels separating the tetrahedra along the c direction appear as white dots, particularly in the thicker parts. These images are very similar to those published by Domengès *et al.* for the corresponding phosphate tungsten bronzes (9).

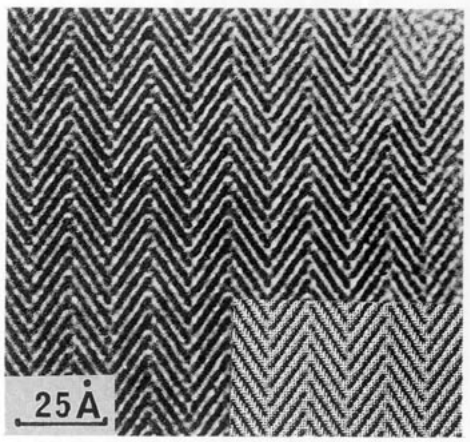

FIG. 3. HREM image of an ordered $(Mo,W)_9O_{25}$ (=[7,$\bar{7}$]) fragment in the [010] projection. A simulated image is inserted in the right bottom corner (defocus, −400 Å; thickness, ~65 Å; spherical aberration, 1.2 mm; aperture radius; 0.41 Å^{-1}).

Variation in the thickness of the ReO_3-type slabs is

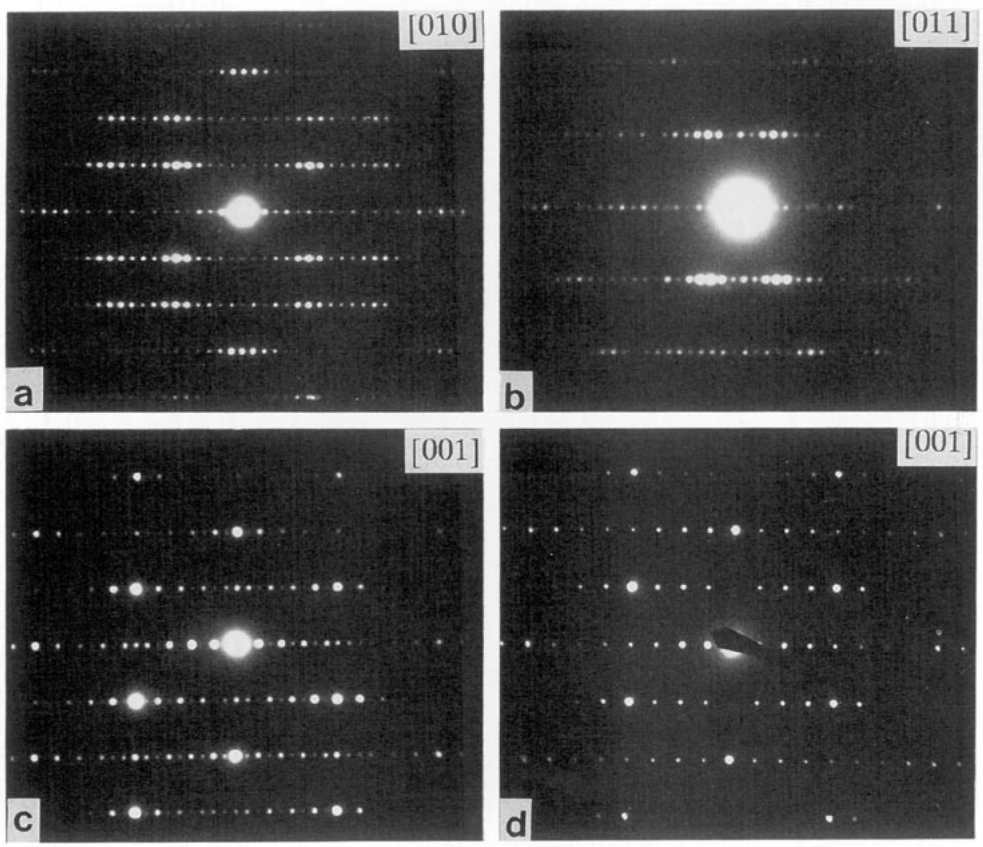

FIG. 2. ED patterns of $(Mo,W)_9O_{25}$ (m = 7) in three projections (a–c) and $(Mo,W)_4O_{11}$ (m = 6) (d).

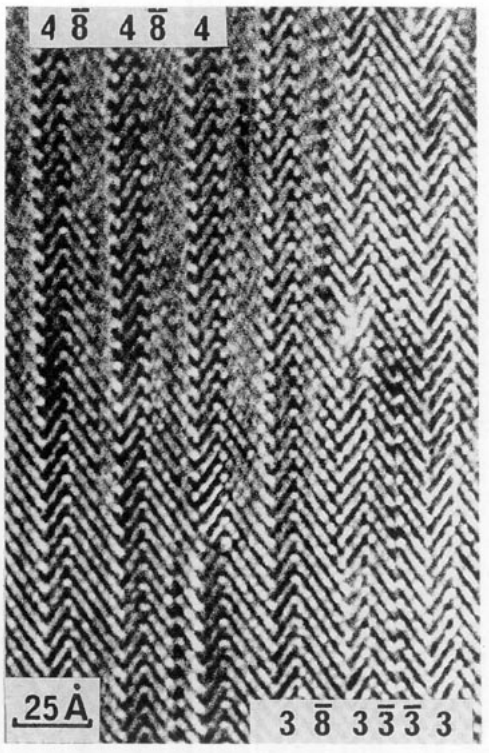

FIG. 4. HREM image of a disordered fragment from sample A. The (probable) widths and orientations of the slabs are indicated.

frequently seen. In addition, the slabs that are wider than seven octahedra are often split into two thinner slabs in parallel orientation in part of their length, thus forming a local intergrowth of the *monoclinic* form (see Fig. 1b). An example of a rather disordered crystal is shown in Fig. 4. Here the width of the slabs varies between $m = 3$ and $m = 9$ and monoclinic intergrowth is also evident.

Figure 5 shows an interesting feature found in a crystal from sample *A*. The upper part of this image is of a regular $[6,\bar{6}]$ type. The lower part, however, is mostly $[5,\bar{7}]$. There is an almost horizontal boundary (marked by arrows) between these two parts where the *c* axis swings by ~5°. A close analysis of the boundary region reveals that there are strings of octahedra that terminate at the boundary, recalling the dislocations at a low-angle grain boundary. A model of the boundary structure is given in Fig. 6. The $[5,\bar{7}]$ structure should have the same length of the unit cell axes as $[6,\bar{6}]$, but the symmetry is monoclinic with a β angle of approximately 95°. The $[5,\bar{7}]$ structure is not regular, however. A careful measurement in the image reveals that approximately 20% of the thicker slabs are wider than the rest and have $m = 8$ instead of 7. These $\bar{8}$ slabs are more or less randomly distributed. They are almost invariably split along part of their length into two thinner slabs in parallel orientation, and thus correspond to an intergrowth of the monoclinic family. The sequence can thus be

$$[\ldots, 5, \bar{7}, 5, \bar{7}, 5, \bar{8}, 5, \bar{7}, 5, \bar{7}, \ldots] \Leftrightarrow$$
$$[\ldots, 5, \bar{7}, 5, \bar{7}, 5, \bar{3}, \bar{3}, 5, \bar{7}, 5, \bar{7}, \ldots].$$

In a couple of places an $\bar{8}$ slab seems to be unsymmetrically split into $\bar{2}$, $\bar{4}$ but only for a short stretch, being unsplit in the surroundings and normally split into $\bar{3}$, $\bar{3}$ further away (Fig. 7). A model of this splitting of an $\bar{8}$ slab is shown in Fig. 1b (to the right).

Evidence of more or less ordered superstructures has been found occasionally. The excerpt from an ED pattern in Fig. 8 is an example. Here, the main spots correspond to a $[6,\bar{6}]$ structure, but fairly sharp reflections between these indicate a superstructure with a ~200 Å repeat. This superstructure is not evident in the corresponding HREM image, however, and its origin is therefore presently unknown.

DISCUSSION

This investigation has shown that homologues of orthorhombic Mo_4O_{11} can be prepared in the ternary Mo–W–O system. So far only one new member, M_9O_{25}, with $m = 7$, has been prepared as a reasonably pure phase, while thicker as well as thinner slabs have been seen in disordered stackings. Only two compositions and essentially one temperature of synthesis have been investigated, however, and it is possible that other homologues can be obtained by extension of these studies to other compositions and temperatures. Such an investigation is in progress.

The fact that sample *A*, with a weighed out composition of $MO_{2.78}$, gave an almost pure sample of M_4O_{11}, while sample C, with a lower average composition of $MO_{2.75}$, gave M_9O_{25}, shows that it is difficult to adjust the oxygen content to fit a particular member of the series. It is probable that the considerably higher tungsten content of sample C favors a higher member. A determination of the actual Mo/W ratio of individual crystallites in relation to their structure has not yet been made but is planned.

It seems to be a fairly general observation that a substitution of tungsten for part of the molybdenum in binary or ternary molybdenum oxides stabilizes wider ReO_3-type elements. It applies to the homologues of monoclinic Mo_4O_{11} ($m = 6$), of which the members with $m = 7$ and 8 have been observed in W-containing samples (5). It is also true for the homologous series Mo_nO_{3n-1} with {102} CS structures where only the members having $n = 8$ and 9 are known in the pure Mo–O system (22), while phases with $n \leq 14$ have been prepared in the Mo–W–O system (21). Finally, it has been found for the homologous series $UO \cdot M_nO_{3n+1}$, with structures comprising slabs of the ReO_3 type of widths proportional to *n*, separated by pen-

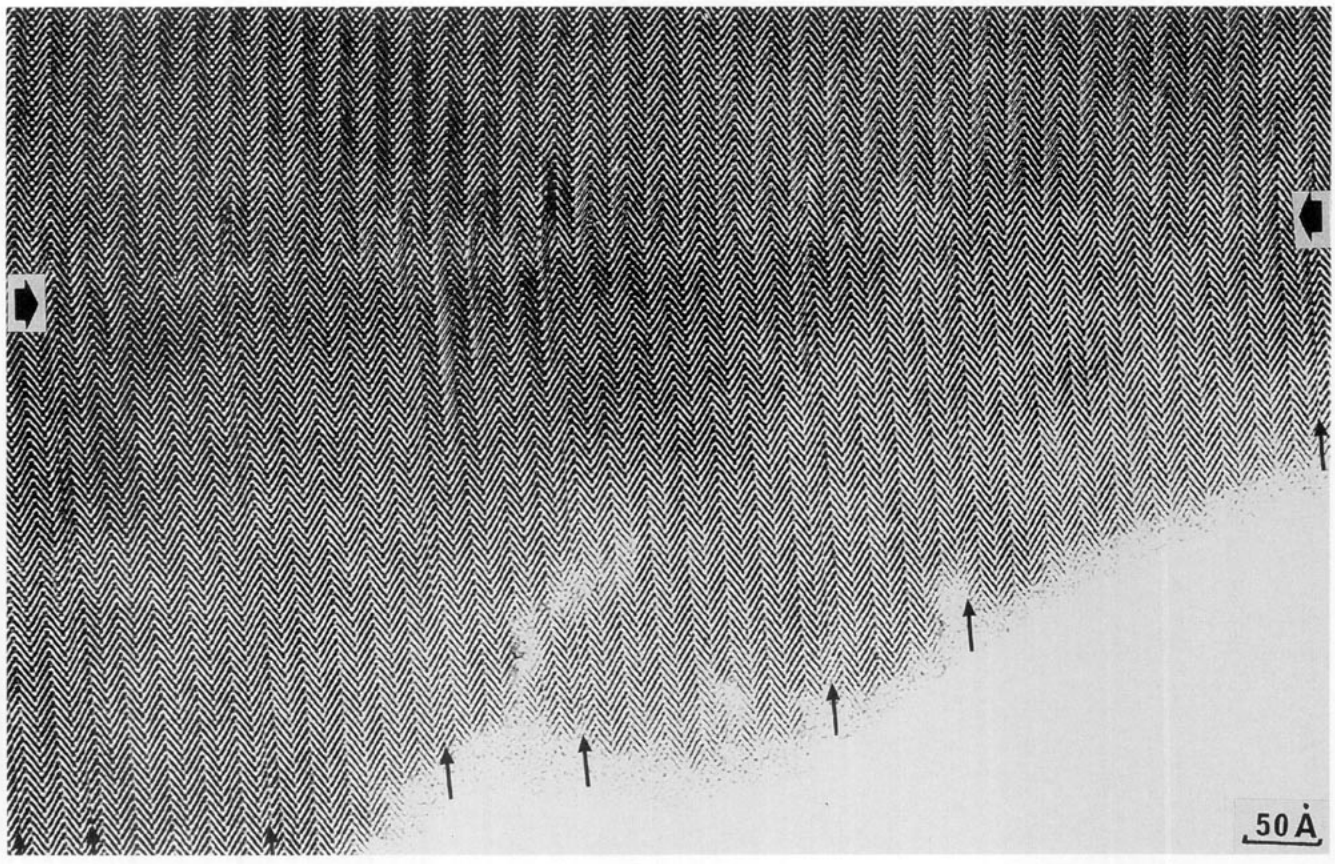

FIG. 5. An HREM image of a crystal from sample A, showing two different $[m,\bar{m}]$ structures seen along [010], coherently intergrown along (001). In the upper part the structure is $[6,\bar{6}]$ and in the lower part it is $[5,\bar{7}]$ with frequent replacement of $\bar{8}$ slabs for $\bar{7}$ in a disordered way (indicated by arrows). The $\bar{8}$ slabs are consistently split into two thinner slabs in monoclinic stacking along part of their length.

tagonal or hexagonal tunnels containing uranium (and oxygen) (23). Here the members with $n = 1$ and 2 form when M = Mo while the phases having n = 3–5 have been obtained with M = (Mo,W).

The formation of practically only $[m,\bar{m}]$ structures in the present high-temperature syntheses, while $[m]$ phases

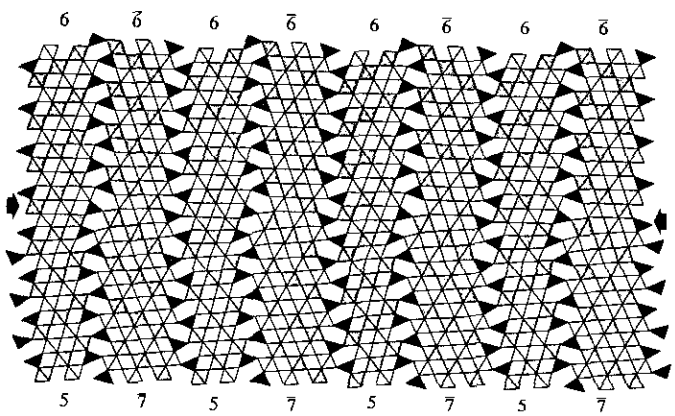

FIG. 6. A model of the boundary structure in Fig. 5.

were obtained in low-temperature experiments (5), is consistent with the fact that Mo_4O_{11}(mon) forms below ~600°C and Mo_4O_{11}(o-rh) above that temperature (1). It is of note that the higher homologues have not been observed before, although the corresponding area of the Mo–W–O system has been the subject of previous phase analysis studies (24, 25). Ekström *et al.* (25) found "Mo_4O_{11}(mon)" in polyphasic samples $Mo_{1-x}W_xO_{2.80}$ with $x \leq 0.05$, which had been heat treated at 600°C, and "Mo_4O_{11}(o-rh)" in samples with $x \leq 0.25$ heated at 600–700°C. No evidence was given that these phases contain tungsten. On the other hand, the phases containing "pentagonal columns" (PCs), namely $(Mo,W)_5O_{14}$ and $(Mo,W)_{17}O_{47}$, which were abundant in their samples, have not been seen in the present study. This is not surprising, however, since these phases have only been obtained at temperatures $\lesssim$700°C (24), considerably lower than those used in the present experiments.

As mentioned above, there is a strong similarity between these phases and the isostructural $MPTB_P$ family of the monophosphate tungsten bronzes and there are many analogies between the observations. Variation in

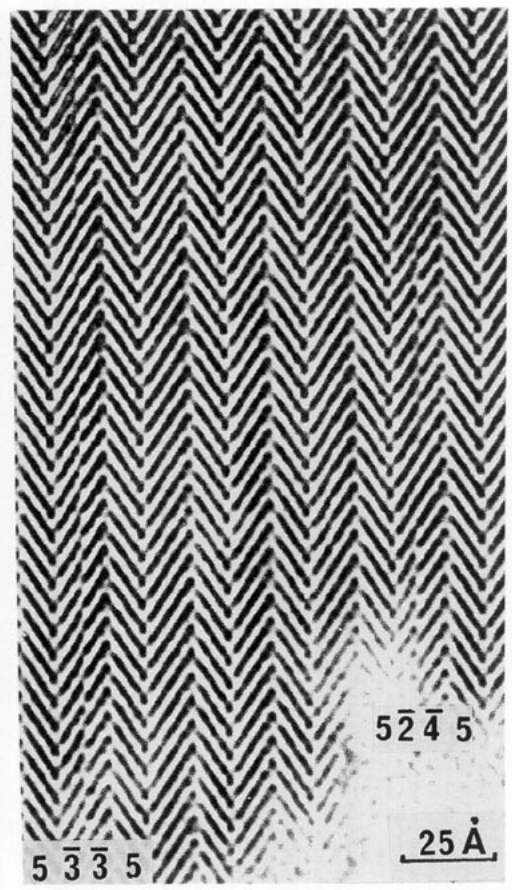

FIG. 7. An enlarged part of Fig. 5 showing the splitting of a wide slab (m = 8) into two thinner slabs in monoclinic orientation.

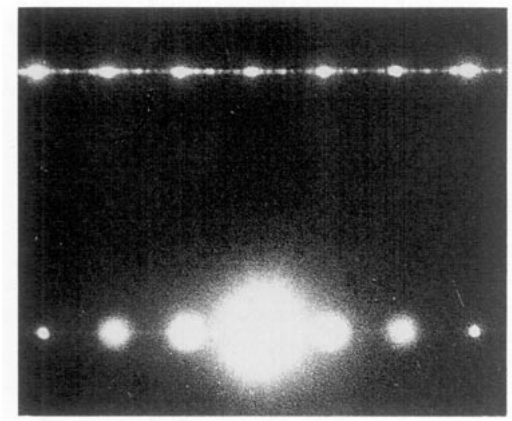

FIG. 8. An ED pattern of a crystal from sample A showing sharp superstructure spots between the strong reflections from a [6,6̄] substructure. The distance between the spots indicates a repeat of ~200 Å in the a direction.

the widths of the ReO_3-type slabs was observed also for the MPTBs (9), and the split of wide slabs of the type described above has also been seen in these mixed oxide phosphates.

The intergrowth along (001) of [6,6̄] and ~[5,7̄] shown in Fig. 5 is a particularly interesting feature. So far it has only been observed once and a detailed analysis and discussion should be postponed until new evidence and, preferably, higher resolution images are available. Some comments may be appropriate here, however. The two structures [6,6̄] and [5,7̄] should ideally have the same length of the a axis. The latter sequence has a monoclinic lattice, however, with a β angle of ~95°. The c axes are therefore inclined to each other by ~5°. It was mentioned above that in the $MPTB_P$ family the [5,5̄] member has not been prepared; instead the [4,6̄] structure forms. We thus have another example of the same type of isomorphism. In the present case both structures exist simultaneously, however.

The [5,7̄] structure occurring here is not regular, but contains frequent replacements of the 7̄ slabs by 8̄ slabs, which are ~1.6 Å wider. A plausible reason for the presence of these wider slabs would be a mismatch of the lattices at the interface amounting to ~2.5%. Since the wider slabs correspond to a slightly higher oxidation state, the splitting of these slabs along part of their length, by which they are reduced, may simply be a compensation for this.

The question of the origin of this intergrowth does not have a simple answer at the present stage. It could be a frozen-in transition state, but it is hard to see which way the transformation then would go. The [6,6̄] structure is more common and regular and should represent a stable state. If that part is the resulting structure in the transformation, it is hard to understand the formation of the ~[5,7̄] part in the first place. It seems more reasonable to believe that this feature is a result of a nucleation or growth defect that has forced the two parts to be inclined. The growth of structures which match epitaxially at the interface and which have closely the same composition has then continued.

ACKNOWLEDGMENT

We thank Mrs. Jaroslava Östberg for assistance with the photographic work. F.P. thanks the Centre National de la Recherche Scientifique for financial support which made his stay at the Arrhenius Laboratory possible. This study forms a part of a research program supported by the Swedish Natural Science Research Council.

REFERENCES

1. L. Kihlborg, *Acta Chem. Scand.* **13,** 954 (1959).
2. L. Kihlborg, *Ark. Kemi* **21,** 365 (1963).
3. A. Magnéli, *Acta Chem. Scand.* **2,** 861 (1948).
4. S. Åsbrink and L. Kihlborg, *Acta Chem. Scand.* **18,** 1571 (1964).

5. F. Portemer, M. Sundberg, L. Kihlborg, and M. Figlarz, *J. Solid State Chem.* **103,** 403 (1993).
6. J. P. Giroult, M. Goreaud, A. Grandin, Ph. Labbé, and B. Raveau, *Acta Crystallogr. Sect. B* **37,** 2139 (1981).
7. A. Benmoussa, Ph. Labbé, D. Groult, and B. Raveau, *J. Solid State Chem.* **44,** 318 (1982).
8. B. Domengès, F. Studer, and B. Raveau, *Mater. Res. Bull.* **18,** 669 (1983).
9. B. Domengès, M. Hervieu, B. Raveau, and R. J. D. Tilley, *J. Solid State Chem.* **54,** 10 (1984).
10. Ph. Labbé, M. Goreaud, and B. Raveau, *J. Solid State Chem.* **61,** 324 (1986).
11. S. L. Wang, C. C. Wang, and K. H. Lii, *J. Solid State Chem.* **82,** 298 (1989).
12. A. Leclaire, H. Chahboun, D. Groult, and B. Raveau, *Z. Kristallogr.* **177,** 277 (1986).
13. A. Benabbas, M. M. Borel, A. Grandin, A. Leclaire, and B. Raveau, *J. Solid State Chem.* **95,** 245 (1991).
14. G. Costentin, M. M. Borel, A. Grandin, and B. Raveau, *Mater Res. Bull.* **26,** 1051 (1991).
15. M. M. Borel, M. Goreaud, A. Grandin, Ph. Labbé, A. Leclaire, and B. Raveau, *Eur. J. Solid State Inorg. Chem.* **28,** 93 (1991).
16. C. Schlenker, J. Dumas, C. Escribe-Filippini, and H. Guyot, *in* "Low-Dimensional Electronic Properties of Molybdenum Bronzes and Oxides" (C. Schlenker, Ed.), pp. 159–257. Kluwer Academic Publishers, Dordrecht, The Netherlands, 1989.
17. M. Sundberg, F. Portemer, B.-O. Marinder, and L. Kihlborg, SCANDEM 93, Lund, Sweden, 9–11 June 1993, Extended Abstracts, pp. 153–154.
18. K.-E. Johansson, T. Palm, and P.-E. Werner, *J. Phys. E.* **13,** 1289 (1980).
19. M. A. O'Keefe, P. R. Buseck, and S. Iijima, *Nature (London)* **274,** 322 (1978).
20. O. G. D'yachenko, V. V. Tabachenko, and M. Sundberg, to be published.
21. A. Magnéli, B. Blomberg-Hansson, L. Kihlborg, and G. Sundkvist, *Acta Chem. Scand.* **9,** 1382 (1955).
22. A. Magnéli, *Nova Acta Regiae Soc. Sci. Ups.* **14**(8) (1950).
23. M. Sundberg and V. V. Tabachenko, *Microsc. Microanal. Microstruct.* **1,** 373 (1990).
24. T. Ekström, *Mater. Res. Bull.* **7,** 19 (1972).
25. T. Ekström, E. Salje, and R. J. D. Tilley, *J. Solid State Chem.* **40,** 75 (1981).